Effect of orbital symmetry on the orientation dependence of strong field tunnelling ionization of nonlinear polyatomic molecules

2011 J. Phys. B: At. Mol. Opt. Phys. 44 035601

(http://iopscience.iop.org/0953-4075/44/3/035601)

J. Phys. B: At. Mol. Opt. Phys. **44** (2011) 035601 (10pp) doi:10.1088/0953-4075/44/3/035601

Effect of orbital symmetry on the orientation dependence of strong field tunnelling ionization of nonlinear polyatomic molecules

Song-Feng Zhao[1,2], Junliang Xu[1], Cheng Jin[1], Anh-Thu Le[1] and C D Lin[1]

[1] J R Macdonald Laboratory, Department of Physics, Kansas State University, Manhattan, KS 66506, USA

[2] Key Laboratory of Atomic and Molecular Physics and Functional Materials of Ganzu Province, College of Physics and Electronic Engineering, Northwest Normal University, Lanzhou 730070, People's Republic of China

E-mail: zhaosf@nwnu.edu.cn

Received 15 October 2010, in final form 16 December 2010
Published 17 January 2011
Online at stacks.iop.org/JPhysB/44/035601

Abstract

In the strong field molecular tunnelling ionization theory (Tong X M 2002 *Phys. Rev.* A **66** 033402), the ionization rate depends on structure parameters of molecules which can be extracted from molecular wavefunctions in the asymptotic region. By using molecular orbitals obtained from standard quantum chemistry packages, we extract these parameters for several selected nonlinear polyatomic molecules. We show that the symmetry properties of the molecular orbital are reflected vividly in the angle-dependent tunnelling ionization rates. The structure parameters for 17 nonlinear molecules have been calculated and tabulated for future applications.

(Some figures in this article are in colour only in the electronic version)

1. Introduction

The dependence of tunnelling ionization rates on the orientation or alignment of molecules is fundamental to the understanding of all strong field phenomena of molecules, including rescattering phenomena, such as high-order harmonic generation (HHG), high-energy photoelectron spectra and nonsequential double ionization of molecules [1–9]. Experimentally such dependence has been reported only for a small number of molecules [10–19]. Since molecules can only be partially oriented or aligned under field-free conditions [20], the measured experimental data have to be analyzed, often with some models, in order to extract the orientation- or alignment-dependent ionization rate for a fixed-in-space molecule. Thus most of the experimental measurements have been limited to linear molecules which can be efficiently aligned by short infrared laser pulses. As experimentalists began to study strong field phenomena of nonlinear polyatomic molecules, one finds that there is little information available even on the tunnelling ionization rates [21–25]. Theoretically, while ionization of nonlinear polyatomic molecules can in principle be obtained by solving the time-dependent Schrödinger equation, such calculations are very time consuming and quite impractical. Considering exposing a nonlinear polyatomic molecule to a linearly polarized infrared laser pulse, the ionization rate or probability will depend on the polar angles (θ, χ), where the angles measure the orientation of one of the major axes of the molecule with respect to the polarization direction of the laser's electric field. Thus the number of calculations for a given molecule for each laser pulse is already quite large. In actual calculations, a simpler method such as the time-dependent density functional theory (TDDFT) [5, 6, 9, 26] has been generalized and applied to a number of nonlinear molecules [27, 28]. Within the single-active-electron (SAE) approximation, the molecular strong field approximation (SFA) [2, 29] has been used for a few nonlinear molecules [30–32]. In these calculations, each orientation angle (θ, χ) requires a new independent calculation. Thus

the calculations are still rather time consuming since many angles are needed. The simplest method for obtaining an orientation-dependent ionization rate is to use the simple molecular tunnelling ionization theory (MO-ADK) [33, 34], which has been applied to many linear molecules [35–41]. The method was generalized to nonlinear polyatomic molecules [42, 43] previously. Extension of the MO-ADK model beyond the SAE approximation was reported in [44, 45].

Using MO-ADK, the angle-dependent ionization rates from each molecular orbital can be obtained analytically if the structure parameters C_{lm} are available. Since different aspects of strong field phenomena, such as HHG, of many nonlinear polyatomic molecules are of interest recently, it is desirable that these parameters be calculated and made available. In table A.1 of the appendix we tabulate such parameters for a list of 17 molecules for future applications. Meanwhile, we demonstrate that angle-dependent tunnelling ionization rates reflect the symmetry of the molecular orbital from which the electron is tunnelling ionized. This relation has been established previously for linear molecules, both theoretically and experimentally. The examples for nonlinear polyatomic molecules studied here are to support this general result. For completeness, in section 2, the basic equations of the MO-ADK theory are briefly reviewed and specific equations that are to be used for calculating molecular tunnelling ionization rates for nonlinear molecules are given. In section 3, after a brief explanation on how the structure parameters C_{lm} are calculated, selected examples of tunnelling ionization rates for some molecules are displayed and compared to the orbital symmetry of the molecular orbital from which the electron is removed. The important theoretical results—the structure parameters C_{lm} and the equilibrium positions of the atoms for the molecules considered—are tabulated in tables A.1 and A.2 of the appendix, respectively. These parameters should be of interest for future study of strong field phenomena of specific molecules. In section 4 we summarize the results and discuss the possible limitations of this work. Due to the complexity of nonlinear polyatomic molecules, clearly the accuracy of the data provided here cannot be easily checked until further study. Still, we prefer to present the tabulated coefficients in order to help motivate experimental studies of strong field physics of nonlinear polyatomic molecules. We anticipate that further theoretical works will be needed when experimental data become available.

2. Theoretical methods

In the MO-ADK theory [33], the asymptotic electronic wavefunction in the molecular frame, in the single-centre expansion approach, can be expressed as

$$\Psi(\mathbf{r}) = \sum_{lm} F_{lm}(r) Y_{lm}(\hat{\mathbf{r}}), \tag{1}$$

with m the magnetic quantum number along the molecular axis, and $Y_{lm}(\hat{\mathbf{r}})$ are the spherical harmonics. The radial wavefunction in the asymptotic region is given in the form

$$F_{lm}(r \to \infty) \approx C_{lm} r^{Z_c/\kappa - 1} \mathrm{e}^{-\kappa r}, \tag{2}$$

where Z_c and C_{lm} are the effective Coulomb charge and the structure parameters of the molecule, respectively. Here $\kappa = \sqrt{2I_p}$, where I_p is the ionization potential. (Atomic units are used throughout this paper unless indicated otherwise.) We first assume that the molecular frame and the laboratory-fixed frame coincide and that the valence electron is released along the field direction. The leading term of each spherical harmonic along this direction is

$$Y_{lm}(\hat{\mathbf{r}}) \simeq Q(l,m) \frac{\sin^{|m|}\theta_e}{2^{|m|}|m|!} \frac{\mathrm{e}^{\mathrm{i}m\chi_e}}{\sqrt{2\pi}}, \tag{3}$$

with

$$Q(l,m) = (-1)^{(m+|m|)/2} \sqrt{\frac{(2l+1)(l+|m|)!}{2(l-|m|)!}}. \tag{4}$$

Here θ_e and χ_e are the angular coordinates of the active electron in the molecular frame. Substituting equations (2) and (3) into equation (1), the electronic wavefunction of a nonlinear molecule can be written as

$$\begin{aligned}\Psi(\mathbf{r}) &\simeq \sum_{lm} C_{lm} Q(l,m) r^{Z_c/\kappa-1} \mathrm{e}^{-\kappa r} \frac{\sin^{|m|}\theta_e}{2^{|m|}|m|!} \frac{\mathrm{e}^{\mathrm{i}m\chi_e}}{\sqrt{2\pi}} \\ &\simeq \sum_{m} B(m) r^{Z_c/\kappa-1} \mathrm{e}^{-\kappa r} \frac{\sin^{|m|}\theta_e}{2^{|m|}|m|!} \frac{\mathrm{e}^{\mathrm{i}m\chi_e}}{\sqrt{2\pi}},\end{aligned} \tag{5}$$

with

$$B(m) = \sum_{l} C_{lm} Q(l,m). \tag{6}$$

The static ionization rate of nonlinear molecules is given by

$$w_{\mathrm{stat}}(F,0) = \sum_{m} \frac{|B(m)|^2}{2^{|m|}|m|!} \frac{1}{\kappa^{2Z_c/\kappa-1}} \left(\frac{2\kappa^3}{F}\right)^{2Z_c/\kappa-|m|-1} \mathrm{e}^{-2\kappa^3/3F} \tag{7}$$

where F is the peak field strength. If $\mathbf{R} \equiv (\phi, \theta, \chi)$ are the Euler angles of the molecular frame with respect to the laboratory-fixed frame, then $B(m)$ in equation (7) can be expressed as

$$B(m') = \sum_{l,m} C_{lm} D^{l}_{m',m}(\mathbf{R}) Q(l,m') \tag{8}$$

with m' being the magnetic quantum number along the field direction, and the Wigner rotation matrix is

$$D^{l}_{m',m}(\mathbf{R}) = \mathrm{e}^{\mathrm{i}m'\phi} d^{l}_{m',m}(\theta) \mathrm{e}^{\mathrm{i}m\chi}. \tag{9}$$

Here, the laboratory-fixed frame and the molecular frame are labelled by (X, Y, Z) and (x, y, z), respectively. The angle between the Z and z axes is θ. ϕ and χ denote rotations around the Z axis and the z axis, respectively. The static ionization rate can be obtained from

$$\begin{aligned}w_{\mathrm{stat}}(F,\mathbf{R}) = \sum_{m'} &\frac{|B(m')|^2}{2^{|m'|}|m'|!} \frac{1}{\kappa^{2Z_c/\kappa-1}} \\ &\times \left(\frac{2\kappa^3}{F}\right)^{2Z_c/\kappa-|m'|-1} \mathrm{e}^{-2\kappa^3/3F}.\end{aligned} \tag{10}$$

Thus once the structure parameters C_{lm} are obtained, the orientation-dependent tunnelling ionization rates can be calculated analytically.

We note that for a linearly polarized laser, the ionization rate does not depend on ϕ. For further analysis, one can also

define χ-averaged static ionization rates as

$$w_{\rm stat}(F,\theta) = \frac{1}{2\pi}\int_0^{2\pi} w_{\rm stat}(F,\phi=0,\theta,\chi){\rm d}\chi. \qquad (11)$$

We will show that the angle-dependent ionization rate resembles closely the electronic density distribution of the active electron. In the molecular frame, the angular distribution of the asymptotic electron density for the active electron can be written as

$$\rho(\theta_e,\chi_e) = \int_{r_1}^{\infty} |\Psi(r,\theta_e,\chi_e)|^2 r^2 {\rm d}r. \qquad (12)$$

For most molecules studied in this paper, r_1 was taken to be around 4 au. For the purpose of comparison we can further define the θ_e-dependent electron density as

$$\rho(\theta_e) = \frac{1}{2\pi}\int_0^{2\pi} \rho(\theta_e,\chi_e){\rm d}\chi_e. \qquad (13)$$

To obtain the C_{lm} coefficients for nonlinear polyatomic molecules, we calculate molecular wavefunctions at the equilibrium geometry from GAUSSIAN [46] using the Hartree–Fock (HF) method and the augmented quadruple-zeta (AUG-cc-pVQZ) basis set where diffuse orbitals have been included. In the asymptotic region, to obtain the C_{lm} coefficients, we fitted each molecular orbital wavefunction to the form of equations (1) and (2). The typical range of r used in the fitting is from 5 to 10 au for small molecules and from 8 to 20 au for larger molecules. Since the electron is mostly ionized from the highest occupied molecular orbital (HOMO) we focus only on ionization from the HOMO in this paper. The fitted C_{lm} coefficients for several selected nonlinear polyatomic molecules are listed in table A.1 of the appendix, together with the experimental vertical ionization energies. With these parameters, using equation (10), the angle-dependent tunnelling ionization rates can be readily calculated.

3. Results

From the derivation of the MO-ADK theory, it is clear that the angle-dependent tunnelling ionization rates are proportional to the electron density in the asymptotic region. If tunnelling ionization is dominated from a particular molecular orbital, then measurement of the angle-dependent ionization rate (or probability for a given laser pulse) would reflect the angular dependence of the molecular orbital in the asymptotic region. If configuration interaction is small, i.e. when the valence electron is well described by a molecular orbital, then the angular dependence of the wavefunction in the inner region and in the outer region should differ little. Under such conditions, the angle-dependent tunnelling ionization rate would reflect the symmetry of the molecular orbital. For linear molecules, such relation has been well established from theories, and from experiments.

In this paper we have obtained the C_{lm} coefficients for the HOMO orbital(s) of 17 nonlinear molecules. Using the Gaussian code [46], we first locate the equilibrium positions of all the atoms in the molecule. The resulting (x, y, z) coordinates of all atoms in each molecule are presented in table

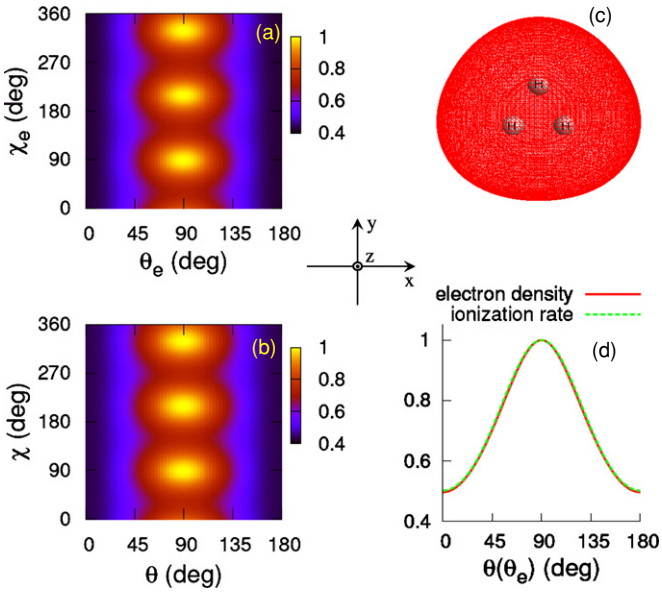

Figure 1. (a) Angular distribution of the normalized asymptotic electron density for H_3^+. (b) Normalized orientation-dependent ionization rate of H_3^+ at laser intensity of 8×10^{14} W cm^{-2}. (c) The isocontour plot of the HOMO wavefunction for H_3^+. (d) Comparison of the normalized θ_e or θ dependence of asymptotic electron density and of the ionization rate for H_3^+. The coordinate system of the body-fixed frame is also shown.

A.2 of the appendix. The C_{lm} coefficients, together with the known experimental vertical ionization energy of the HOMO, are listed in table A.1 of the appendix. Note that in tunnelling ionization, it is the electron density distribution of the HOMO that is important, even though in some cases the HOMO-1 or even HOMO-2 can contribute if they just lie slightly below the HOMO. In the following, we use the fitted C_{lm} coefficients for selective nonlinear polyatomic molecules to obtain angle-dependent tunnelling ionization rates and compare them to the shape of the molecule orbital from which the electron is removed. We emphasize that in using equation (10) to calculate the ionization rates, we always use experimental ionization energy. In the fitting of the C_{lm} coefficients, we use the calculated binding energy from the GAUSSIAN code to calculate κ in equation (2).

(1) H_3^+. For the simplest nonlinear molecule H_3^+, we arrange three H's on the xy plane. The coordinates of three atoms at the equilibrium configuration are given in table A.2 of the appendix. The contour plot of the HOMO orbital is shown in figure 1(c). The angular distributions of the asymptotic electron density of the HOMO in the molecular frame are shown in figure 1(a) and the calculated tunnelling ionization rates from the MO-ADK theory are shown in figure 1(b), respectively. In figure 1(a), the electron density peaks at $\theta_e = 90^\circ$, and on the xy plane, the density has the C_3 symmetry. The ionization rate was calculated with a laser intensity of 8×10^{14} W cm^{-2}. For simplicity, all electron densities and ionization rates presented in this paper are normalized to 1.0 at the peak. Note that the orientation-dependent ionization rate calculated from MO-ADK theory, as shown in figure 1(b), indeed resembles closely the electron

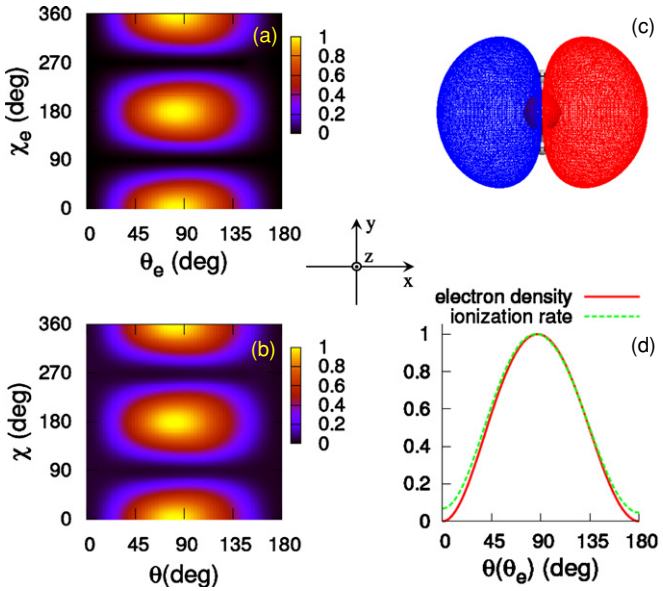

Figure 2. (a) Angular distribution of the normalized asymptotic electron density for H_2O. (b) Normalized orientation-dependent ionization rate of H_2O at laser intensity of 8×10^{13} W cm^{-2}. (c) The isocontour plot of the HOMO wavefunction for H_2O. The sign of the HOMO wavefunction is indicated by different colours, i.e. red denotes positive sign and blue denotes negative sign. (d) Comparison of the normalized θ_e or θ dependence of the asymptotic electron density and ionization rate for H_2O. The x, y and z axes of the body-fixed frame are also shown.

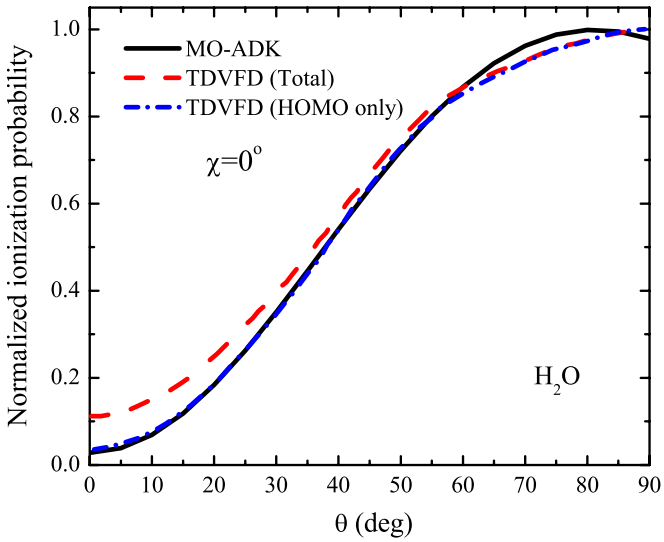

Figure 3. The normalized ionization probability of H_2O calculated for 800 nm lasers at intensity of 5×10^{13} W cm^{-2}. The sine-squared pulse with total duration of 20 optical cycles is used in both calculations. TDVFD results are from [28]

density plotted in figure 1(a). To demonstrate the quantitative agreement, we compare in figure 1(d) the asymptotic electron densities and the ionization rates after they are integrated over the azimuthal angle. By normalizing the two curves at the peak, we can see the good agreement in the resulting polar angle (θ or θ_e) dependence.

The orientation dependence of tunnelling ionization rates of H_3^+ has been reported in [25]. In this experiment, the deduced orientation dependence of single ionization was found to change significantly with the pulse duration (7 fs versus 40 fs). Since the experiment does not measure the orientation-dependent tunnelling ionization directly, and the molecular ions are not in the ground vibrational state, direct comparison of this calculation with the experiment is not possible at this time.

(2) *H_2O*. For the planar H_2O molecule, we choose the molecule to lie on the yz plane, with the O atom along the z axis. The HOMO orbital of H_2O contains a nodal plane (i.e. yz plane) (see figure 2(c)). The electron density and tunnelling ionization rate, shown in polar coordinates in figures 2(a) and (b), respectively, are seen to be very similar. The θ dependence of the ionization rate agrees well with the asymptotic electron density also, as shown in figure 2(d).

We can compare the ionization rate from MO-ADK theory with other theoretical results. Figure 3 compares the θ dependence of the normalized ionization probability of H_2O at $\chi = 0^\circ$ from MO-ADK with those using the TDVFD method [28]. Clearly, the θ dependence of the ionization probabilities from the two methods agree well with each other, especially if one directly compares ionization probabilities contributed from the HOMO orbital. This comparison demonstrates that reliable orientation-dependent tunnelling ionization rates can be obtained from the simple MO-ADK theory for nonlinear molecules. Such agreement has been demonstrated previously for linear molecules.

(3) *C_2H_6*. We next consider the ethane molecule. The coordinates of the atoms for ethane in equilibrium are given in table A.2 of the appendix. Here the two carbon atoms lie along the z axis. There are three H's forming an equilateral triangle, one lying on the $z = 1.164$ plane, and another on the $z = -1.164$ plane. The two triangles are located symmetrically (see figure 4(a)). From table A.1 of the appendix we note that there are two degenerate HOMOs for ethane, they are shown in figures 4(b) and (f), respectively. The angular distributions of the asymptotic electron densities for the two HOMOs are shown in figures 4(c) and (g) and the angle-dependent tunnelling ionization rates are shown in figures 4(d) and (h), respectively. The results demonstrate that the orientation dependence of tunnelling ionization rates follows well the electronic density of the HOMO orbitals.

(4) *Isomers of C_4H_{10}*—butane versus isobutane. Here we consider the two isomers of C_4H_{10}, butane and isobutane. They have identical chemical compositions but the atoms are arranged differently and thus their HOMOs are also quite different, as depicted in the top two rows in figure 5. The HOMOs are plotted such that the z axis is coming out of the plane. The electron density plots are shown in the third row. It is clearly seen that the charge density of the HOMO for butane is mostly lying on the xy plane ($\theta_e = 90^\circ$). The MO-ADK tunnelling ionization rates are peaked in the same angular range. For isobutane, the HOMO is quite different. The same xy plane is a nodal

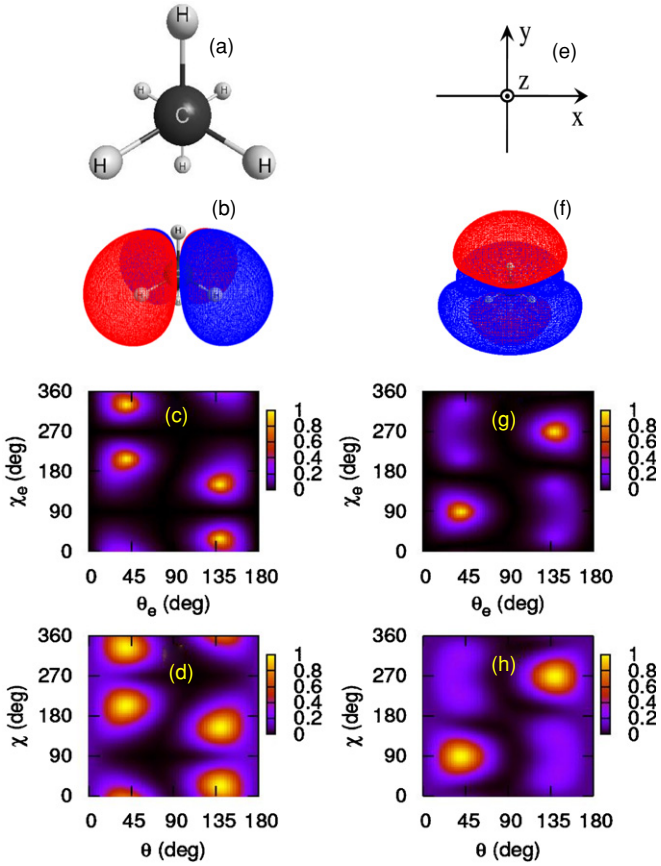

Figure 4. (a) Atomic configuration of C_2H_6. The second carbon is behind the first one along the z axis. The body-fixed axes are defined in (e). The second row gives the isocontour plot of the HOMO1 (b) and the HOMO2 (f). Red is for positive and blue is for negative wavefunction. The angular distributions of the asymptotic electron density and the orientation-dependent tunnelling ionization rates for HOMO1 and HOMO2 are shown below each orbital, respectively. Laser intensity of 5×10^{13} W cm^{-2} was used in the calculation.

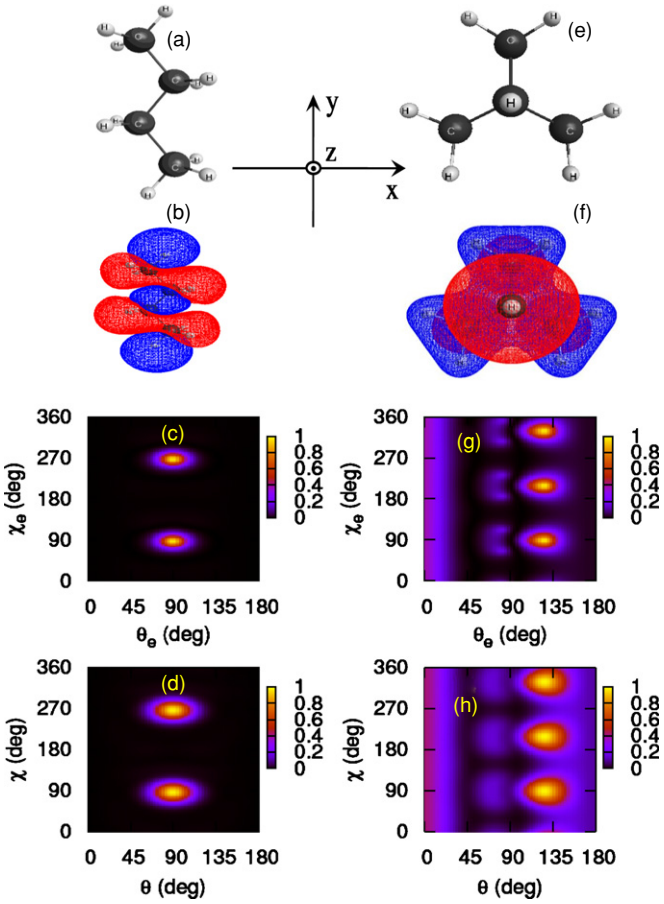

Figure 5. Molecular geometries of butane (a) and isobutane (e). Below each isomer, the HOMO wavefunction, the angular distributions of the HOMO and the orientation-dependent ionization rates are shown respectively. Laser intensity of 3×10^{13} W cm^{-2} was used.

plane. The electron density peaks at $\theta_e = 0$ as well as at θ_e near 130° where the latter has three-fold symmetry in χ_e. Figures 5(d) and (h) show that the calculated MO-ADK rates for both isomers reflect the symmetry of the molecular orbitals (see figures 5(c) and (g)) quite well.

(5) *CH_2Cl_2*, *$CHCl_3$* and *CCl_4*. These three molecules can be considered as resulting from replacing the hydrogen atoms in the methane molecule (CH_4) by two, three and four chlorine atoms, respectively. The shapes of electron density distributions of the HOMO for each of the three molecules, CH_2Cl_2, $CHCl_3$ and CCl_4, are shown along the first row in figure 6 using the coordinate system where the z axis is pointing out of the plane. Using such a frame, the nodal surfaces can be readily visualized, such that the symmetry of the electron cloud is clearly displayed. The angular dependence of the MO-ADK tunnelling ionization rates expressed in this coordinate frame shown in the bottom row agrees well with the angular distributions of the molecular orbitals in the middle row faithfully (see figure 6). For the precise positions of the atoms in this coordinate frame, the readers should consult the data in table A.2 of the appendix.

4. Summary and discussion

In this paper we have obtained the structure parameters C_{lm} for a list of 17 nonlinear polyatomic molecules using wavefunctions obtained from the GAUSSIAN [46] structure code. These structure parameters can be used to obtain strong-field tunnelling ionization rates within the MO-ADK model. Since tunnelling ionization is the first step in all nonlinear interactions of molecules in strong fields, with the available C_{lm}, angle-dependent tunnelling ionization rates can be readily calculated. We have further confirmed that the angular dependence of ionization rates resembles closely the shape of the molecular orbital from which the electron was removed.

Clearly the results presented in this paper have many limitations. Strong field ionization from a polyatomic molecule is expected to be quite complicated. What we have included here are only for ionization from the HOMO of each molecule for atoms at their equilibrium configurations. For most polyatomic molecules there are many inner orbitals that have binding energies not too far from the binding energy of the HOMO and these orbitals are expected to contribute to tunnelling ionization, especially for angles where tunnelling from the HOMO is small. The contributions of inner orbitals

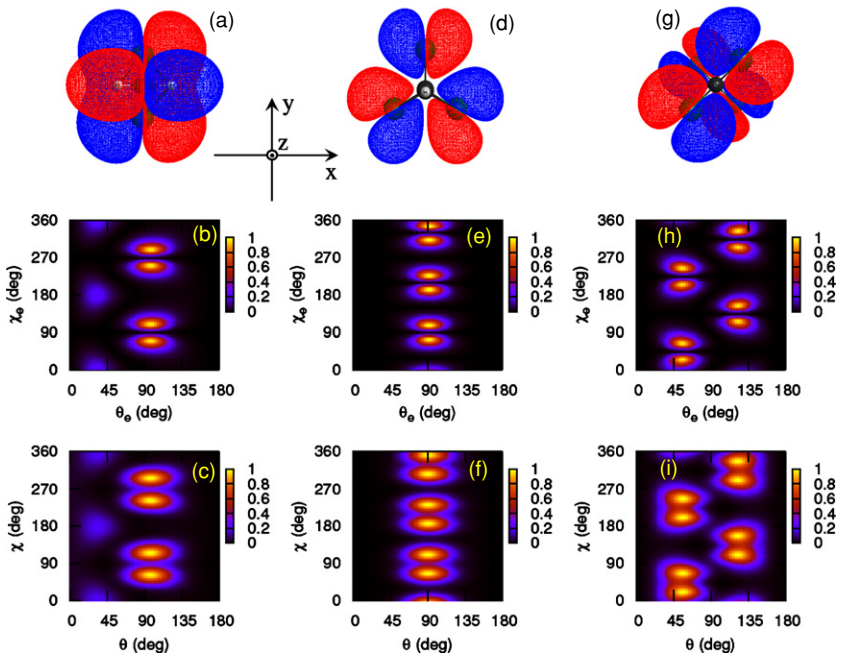

Figure 6. The isocontour plot of the HOMO wavefunctions is shown in the first row, in the order CH_2Cl_2, $CHCl_3$ and CCl_4. The angular distributions of the HOMO and the orientation-dependent ionization rates for each molecule are shown below, respectively. Laser intensity of 5×10^{13} W cm^{-2} was used.

have been investigated so far only for linear molecules. For example, tunnelling ionization rates from HOMO, HOMO-1 and HOMO-2 have been investigated, e.g. see figure 24(b) for N_2 and figure 21 for CO_2, respectively, of [1]. (See also figure 3 for H_2O.) There are no experimental data to directly check the accuracy of the calculated ionization rates from these well-studied molecules. There is, however, evidence of contributions of inner-shell orbitals in HHG in N_2 when the molecules are aligned perpendicular to the laser's polarization, as shown experimentally [47] and theoretically [48]. There is also evidence of inner-shell contributions for HHG from CO_2 molecules when the molecules are aligned parallel to laser's polarization[49]. In both cases, clear evidence of contributions of inner-shell orbitals occur at angles where tunnelling ionization rates from the HOMO orbital are very small. For other angles the HOMO orbital is still dominant since tunnelling is highly selective with respect to the binding energy of the orbital. As the laser intensity increases, the dominance of the HOMO becomes weaker. However, at higher laser intensities other factors like ionization saturation or depletion can come into play which will make the interpretation of data even more complicated for polyatomic molecules.

Another issue that should be addressed is the accuracy of the C_{lm} coefficients calculated for larger molecules. The wavefunctions for the HOMO orbitals in this work have been calculated from GAUSSIAN [46] using the basis set described in section 2. These wavefunctions are not accurate in the asymptotic region, even if many more diffuse orbitals are added in the basis set. The result is that the C_{lm} coefficients may not be highly accurate. Methods have been developed in [34] where an accurate asymptotic wavefunction can be accurately calculated. The method has been applied to linear molecules. It can also be applied to nonlinear molecules except that the computation is much larger. The latter can only be performed one molecule a time when it is needed. Still, the results (figure 2 of [34]) show that the alignment dependence remains nearly the same even after more accurate C_{lm} coefficients are used, despite that the tunnelling rates can be changed somewhat. Thus we are optimistic that the coefficients tabulated here are sufficient to provide a first-order estimate of strong field ionization of nonlinear polyatomic molecules. They are to be used to motivate experimental studies of more complex polyatomic molecules. Only through such experimental studies will more elaborate theoretical investigations of strong field ionization of polyatomic molecules follow.

Acknowledgments

This work was supported in part by Chemical Sciences, Geosciences and Biosciences Division, Office of Basic Energy Sciences, Office of Science, US Department of Energy. SFZ was also supported by the National Natural Science Foundation of China under grant no 11044007, the Specialized Research Fund for the Doctoral Program of Higher Education of China under grant no 20096203110001 and the Foundation of Northwest Normal University under grant no NWNU-KJCXGC-03-70.

Appendix

The newly fitted C_{lm} structure coefficients and the experimental vertical ionization energies for several selected nonlinear polyatomic molecules are tabulated in table A.1. The *x, y, z* coordinates (in Angstroms) of all atoms in each

Table 1. Fitted C_{lm} structure coefficients for several nonlinear polyatomic molecules. The degenerate HOMOs are denoted by HOMO1, HOMO2 and HOMO3. The experimental vertical ionization energies are also listed.

Molecule	Orbitals	I_p (eV)	C_{lm}										
C_2H_4		10.51	$C_{1\pm1}$	$C_{3\pm1}$									
	$1b_{3u}$(HOMO)		∓1.08	∓0.20									
C_6H_6		9.25	$C_{2\pm1}$	$C_{4\pm1}$									
	$1e_{1g}$(HOMO1)		∓1.40	±0.33									
	$1e_{1g}$(HOMO2)		1.40i	-0.33i									
H_3^+		32.33	C_{00}	C_{20}	$C_{3\pm3}$	C_{40}	$C_{5\pm3}$						
	$1a_1'$(HOMO)		4.75	-0.47	-0.12i	0.02	0.01i						
H_2O		12.60	$C_{1\pm1}$	$C_{2\pm1}$	$C_{3\pm1}$	$C_{3\pm3}$	$C_{4\pm1}$	$C_{4\pm3}$	$C_{5\pm3}$	$C_{5\pm5}$			
	$1b_1$(HOMO)		∓1.40	∓0.05	∓0.02	±0.06	∓0.01	∓0.03	±0.01	∓0.01			
SO_2		12.34	C_{00}	C_{10}	C_{20}	$C_{2\pm2}$	C_{30}	$C_{3\pm2}$	C_{40}	$C_{4\pm2}$	$C_{4\pm4}$	C_{50}	$C_{5\pm2}$
	$8a_1$(HOMO)		2.96	-0.74	1.28	-0.06	0.84	0.70	-0.32	-0.29	0.05	-0.05	-0.07
			$C_{5\pm4}$	C_{60}	$C_{6\pm2}$	$C_{6\pm4}$							
	–		-0.12	0.07	0.06	0.05							
N_2O_4		11.50	C_{00}	C_{20}	$C_{2\pm2}$	C_{40}	$C_{4\pm2}$	$C_{4\pm4}$	C_{60}	$C_{6\pm2}$	$C_{6\pm4}$	C_{80}	$C_{8\pm4}$
	$6a_g$(HOMO)		-4.05	-4.63	0.28	0.15	1.99	-0.03	0.67	0.66	-0.20	0.04	-0.07
NH_3		10.20	C_{00}	C_{10}	C_{20}	C_{30}							
	$3a_1$(HOMO)		0.08	1.38	0.11	-0.07							
CH_4		12.60	$C_{1\pm1}$	$C_{2\pm1}$	$C_{3\pm1}$	$C_{3\pm3}$	$C_{4\pm1}$	$C_{4\pm3}$					
	$1t_2$(HOMO1)		∓2.23	0.80i	∓0.13	±0.17	-0.04i	0.10i					
	$1t_2$(HOMO2)		2.23i	∓0.80	0.13i	0.17i	±0.04	±0.10					
			C_{10}	$C_{2\pm2}$	C_{30}	$C_{4\pm2}$							
	$1t_2$(HOMO3)		3.16	∓0.80i	-0.30	∓0.11i							
C_2H_6		11.50	$C_{2\pm1}$	$C_{2\pm2}$	$C_{4\pm1}$	$C_{4\pm2}$	$C_{6\pm1}$	$C_{6\pm2}$	$C_{6\pm4}$				
	$1e_g$(HOMO1)		∓2.77	±0.90i	∓0.48	±0.54i	±0.04	±0.06i	±0.06i				
	$1e_g$(HOMO2)		2.77i	-0.90	0.48i	-0.54	-0.04i	-0.06	0.06				
C_3H_8		11.00	$C_{1\pm1}$	$C_{2\pm1}$	$C_{3\pm1}$	$C_{3\pm3}$	$C_{4\pm1}$	$C_{4\pm3}$	$C_{5\pm1}$	$C_{5\pm3}$	$C_{5\pm5}$	$C_{6\pm3}$	$C_{6\pm5}$
	$2b_1$(HOMO)		±1.00	∓2.70	∓0.64	∓1.49	±0.06	±0.75	∓0.18	∓0.24	±0.18	∓0.08	∓0.08
CH_3Cl		11.30	$C_{1\pm1}$	$C_{2\pm1}$	$C_{2\pm2}$	$C_{3\pm1}$	$C_{3\pm2}$	$C_{4\pm1}$	$C_{4\pm2}$	$C_{5\pm1}$	$C_{5\pm2}$	$C_{6\pm1}$	$C_{6\pm2}$
	3e(HOMO1)		0.58i	1.72i	0.21	-0.36i	-0.27	0.54i	0.24	-0.13i	-0.17	0.06i	0.09
	3e(HOMO2)		∓0.58	∓1.72	∓0.21i	±0.36	±0.27i	∓0.54	∓0.24i	±0.13	±0.17i	∓0.06	∓0.09i

Table 1. (Continued.)

Molecule	Orbitals	I_p (eV)	C_{lm}						
C_4H_{10} (butane)		10.60	C_{00}	C_{20}	$C_{2\pm2}$	C_{40}	$C_{4\pm2}$	$C_{4\pm4}$	C_{60}
	$7a_g$(HOMO)		−3.91	5.04	6.96±1.00i	−3.18	−3.05∓0.30i	−4.48∓1.00i	1.11
			$C_{6\pm2}$	$C_{6\pm4}$	$C_{6\pm6}$	C_{80}	$C_{8\pm2}$	$C_{8\pm4}$	
	–		1.06∓0.03i	1.09±0.04i	1.66±0.19i	−0.30	−0.29	−0.28	
C_4H_{10} (isobutane)		11.13	C_{00}	C_{10}	C_{20}	C_{30}	$C_{3\pm3}$	C_{40}	$C_{4\pm3}$
	$6a_1$(HOMO)		2.47	−2.64	2.69	2.82	−0.48i	−0.73	1.08i
			C_{50}	$C_{5\pm3}$	C_{60}	$C_{6\pm3}$	$C_{6\pm6}$	C_{70}	$C_{7\pm3}$
	–		−0.22	−0.36i	0.15	−0.05i	−0.21	0.02	0.03i
			$C_{7\pm6}$						
	–		0.04						
CH_2Cl_2		11.33	$C_{1\pm1}$	$C_{2\pm1}$	$C_{3\pm1}$	$C_{3\pm3}$	$C_{4\pm1}$	$C_{4\pm3}$	$C_{5\pm1}$
	$3b_1$(HOMO)		∓1.50	±1.37	±1.18	±2.63	±0.07	∓0.43	∓0.01
			$C_{5\pm3}$	$C_{5\pm5}$	$C_{6\pm1}$	$C_{6\pm3}$	$C_{6\pm5}$	$C_{7\pm3}$	$C_{7\pm5}$
	–		∓0.26	∓0.85	±0.05	±0.16	±0.18	±0.06	±0.09
$CHCl_3$		11.37	$C_{3\pm3}$	$C_{4\pm3}$	$C_{5\pm3}$	$C_{6\pm6}$	$C_{7\pm3}$		
	$2a_2$(HOMO)		±4.78	∓0.31	∓0.90	∓1.18i	±0.20		
CCl_4		11.47	$C_{3\pm2}$	$C_{4\pm4}$	$C_{6\pm4}$	$C_{7\pm2}$	$C_{7\pm6}$	$C_{9\pm6}$	$C_{10\pm8}$
	$2t_1$(HOMO1)		5.08	∓2.68i	∓1.40i	−0.30	−0.83	−0.32	±0.23i
			$C_{3\pm1}$	$C_{3\pm3}$	$C_{4\pm1}$	$C_{4\pm3}$	$C_{6\pm1}$	$C_{6\pm3}$	$C_{6\pm5}$
	$2t_1$(HOMO2)		±4.02	±3.11	−2.51i	−0.95i	0.61i	−0.94i	−0.82i
			$C_{7\pm1}$	$C_{7\pm3}$	$C_{7\pm5}$	$C_{7\pm7}$			
	–		∓0.54	∓0.51	∓0.35	∓0.26			
			$C_{3\pm1}$	$C_{3\pm3}$	$C_{4\pm1}$	$C_{4\pm3}$	$C_{6\pm1}$	$C_{6\pm3}$	$C_{6\pm5}$
	$2t_1$(HOMO3)		−4.02i	3.11i	±2.51	∓0.95	∓0.61	∓0.94	±0.82
			$C_{7\pm1}$	$C_{7\pm3}$	$C_{7\pm5}$	$C_{7\pm7}$			
	–		0.54i	−0.51i	0.35i	−0.26i			
SF_6		15.69	$C_{4\pm1}$	$C_{4\pm3}$	$C_{6\pm1}$	$C_{6\pm3}$	$C_{6\pm5}$	$C_{8\pm1}$	$C_{8\pm3}$
	$1t_{1g}$(HOMO1)		∓7.98	±3.01	∓0.55	∓0.87	±0.75	∓0.37	±0.13
			$C_{8\pm5}$	$C_{8\pm7}$					
	–		∓0.12	±0.10					
			$C_{4\pm1}$	$C_{4\pm3}$	$C_{6\pm1}$	$C_{6\pm3}$	$C_{6\pm5}$	$C_{8\pm1}$	$C_{8\pm3}$
	$1t_{1g}$(HOMO2)		7.98i	3.01i	0.55i	−0.87i	−0.75i	0.37i	0.13i
			$C_{8\pm5}$	$C_{8\pm7}$					
	–		0.12i	0.10i					
			$C_{4\pm4}$	$C_{6\pm4}$	$C_{8\pm4}$	$C_{8\pm8}$	$C_{10\pm4}$	$C_{10\pm8}$	
	$1t_{1g}$(HOMO3)		±8.53i	∓1.28i	±0.13i	±0.40i	∓0.01i	∓0.02i	

Table 2. The *x*, *y*, *z* coordinates (in Angstroms) of atoms for several selected nonlinear polyatomic molecules at equilibrium calculated from the GAUSSIAN packages.

Molecule	Atoms	*x*	*y*	*z*	Molecule	Atoms	*x*	*y*	*z*
H_3^+	H	0.000 000	0.504 258	0.000 000	H_2O	O	0.000 000	0.000 000	0.117 287
	H	0.436 700	−0.252 129	0.000 000		H	0.000 000	0.757 118	−0.469 148
	H	−0.436 700	−0.252 129	0.000 000		H	0.000 000	−0.757 118	−0.469 148
SO_2	S	0.000 000	0.000 000	0.370 459	NH_3	N	0.000 000	0.000 000	0.106 104
	O	0.000 000	1.262 322	−0.370 459		H	0.000 000	0.933 095	−0.247 577
	O	0.000 000	−1.262 322	−0.370 459		H	−0.808 084	−0.466 548	−0.247 577
						H	0.808 084	−0.466 548	−0.247 577
CH_4	C	0.000 000	0.000 000	0.000 000	CH_3Cl	C	0.000 000	0.000 000	−1.138 765
	H	0.627 447	0.627 447	0.627 447		Cl	0.000 000	0.000 000	0.664 141
	H	−0.627 447	−0.627 447	0.627 447		H	0.000 000	1.033 456	−1.485 933
	H	−0.627 447	0.627 447	−0.627 447		H	0.894 999	−0.516 728	−1.485 933
	H	0.627 447	−0.627 447	−0.627 447		H	−0.894 999	−0.516 728	−1.485 933
CH_2Cl_2	C	0.000 000	0.000 000	0.764 025	$CHCl_3$	C	0.000 000	0.000 000	0.454 858
	Cl	0.000 000	1.486 186	−0.215 774		H	0.000 000	0.000 000	1.535 158
	Cl	0.000 000	−1.486 186	−0.215 774		Cl	0.000 000	1.693 346	−0.083 614
	H	−0.904 322	0.000 000	1.376 082		Cl	1.466 481	−0.846 673	−0.083 614
	H	0.904 322	0.000 000	1.376 082		Cl	−1.466 481	−0.846 673	−0.083 614
CCl_4	C	0.000 000	0.000 000	0.000 000	C_2H_4	C	0.000 000	0.000 000	0.669 500
	Cl	1.028 319	1.028 319	1.028 319		C	0.000 000	0.000 000	−0.669 500
	Cl	−1.028 319	−1.028 319	1.028 319		H	0.000 000	0.928 797	1.234 217
	Cl	−1.028 319	1.028 319	−1.028 319		H	0.000 000	−0.928 797	1.234 217
	Cl	1.028 319	−1.028 319	−1.028 319		H	0.000 000	0.928 797	−1.234 217
						H	0.000 000	−0.928 797	−1.234 217
N_2O_4	N	0.000 000	0.000 000	0.901 500	SF_6	S	0.000 000	0.000 000	0.000 000
	N	0.000 000	0.000 000	−0.901 500		F	0.000 000	0.000 000	1.589 634
	O	0.000 000	1.094 466	1.357 082		F	0.000 000	1.589 634	0.000 000
	O	0.000 000	−1.094 466	1.357 082		F	0.000 000	0.000 000	−1.589 634
	O	0.000 000	1.094 466	−1.357 082		F	−1.589 634	0.000 000	0.000 000
	O	0.000 000	−1.094 466	−1.357 082		F	1.589 634	0.000 000	0.000 000
						F	0.000 000	−1.589 634	0.000 000
C_2H_6	C	0.000 000	0.000 000	0.765 450	C_3H_8	C	0.000 000	0.000 000	0.585 916
	C	0.000 000	0.000 000	−0.765 450		C	0.000 000	1.277 033	−0.259 559
	H	0.000 000	1.021 056	1.164 048		C	0.000 000	−1.277 033	−0.259 559
	H	−0.884 260	−0.510 528	1.164 048		H	−0.877 145	0.000 000	1.247 552
	H	0.884 260	−0.510 528	1.164 048		H	0.877 145	0.000 000	1.247 552
	H	0.000 000	−1.021 056	−1.164 048		H	0.000 000	2.176 351	0.367 167
	H	−0.884 260	0.510 528	−1.164 048		H	0.000 000	−2.176 351	0.367 167
	H	0.884 260	0.510 528	−1.164 048		H	−0.884 308	1.323 067	−0.907 556
						H	−0.884 308	−1.323 067	−0.907 556
						H	0.884 308	1.323 067	−0.907 556
						H	0.884 308	−1.323 067	−0.907 556
C_6H_6	C	0.000 000	1.390 970	0.000 000					
	C	1.204 615	0.695 485	0.000 000					
	C	1.204 615	−0.695 485	0.000 000					
	C	0.000 000	−1.390 970	0.000 000					
	C	−1.204 615	−0.695 485	0.000 000					
	C	−1.204 615	0.695 485	0.000 000					
	H	0.000 000	2.473 265	0.000 000					
	H	2.141 910	1.236 632	0.000 000					
	H	2.141 910	−1.236 633	0.000 000					
	H	0.000 000	−2.473 265	0.000 000					
	H	−2.141 910	−1.236 633	0.000 000					
	H	−2.141 910	1.236 633	0.000 000					
C_4H_{10} (butane)	C	0.421 038	0.641 014	0.000 000	C_4H_{10} (isobutane)	C	0.000 000	0.000 000	0.372 704
	C	−0.421 038	−0.641 014	0.000 000		H	0.000 000	0.000 000	1.473 239
	C	−0.421 038	1.920 196	0.000 000		C	0.000 000	1.462 092	−0.095 841
	C	0.421 038	−1.920 196	0.000 000		H	0.000 000	1.521 097	−1.192 338
	H	1.083 920	0.637 337	0.877 525		H	−0.886 216	1.997 579	0.265 449
	H	−1.083 920	−0.637 337	−0.877 525		H	0.886 216	1.997 579	0.265 449
	H	1.083 920	0.637 337	−0.877 525		C	1.266 209	−0.731 046	−0.095 841

Table 2. (Continued.)

Molecule	Atoms	x	y	z	Molecule	Atoms	x	y	z
	H	−1.083 920	−0.637 337	0.877 525		H	1.317 309	−0.760 549	−1.192 338
	H	0.208 625	2.817 198	0.000 000		H	2.173 062	−0.231 304	0.265 449
	H	−0.208 625	−2.817 198	0.000 000		H	1.286 846	−1.766 275	0.265 449
	H	−1.068 590	1.968 623	0.884 360		C	−1.266 209	−0.731 046	−0.095 841
	H	1.068 590	−1.968 623	−0.884 360		H	−1.317 309	−0.760 549	−1.192 338
	H	−1.068 590	1.968 623	−0.884 360		H	−1.286 846	−1.766 275	0.265 449
	H	1.068 590	−1.968 623	0.884 360		H	−2.173 062	−0.231 304	0.265 449

nonlinear molecule used in the present structure calculations are also presented in table A.2.

References

[1] Lin C D, Le A T, Chen Z, Morishita T and Lucchese R 2010 *J. Phys. B: At. Mol. Opt. Phys.* **43** 122001
[2] Kjeldsen T K and Madsen L B 2004 *J. Phys. B: At. Mol. Opt. Phys.* **37** 2033
[3] Abu-samha M and Madsen L B 2009 *Phys. Rev.* A **80** 023401
[4] Spanner M and Patchkovskii S 2009 *Phys. Rev.* A **80** 063411
[5] Son S K and Chu S I 2009 *Phys. Rev.* A **80** 011403
[6] Telnov D A and Chu S I 2009 *Phys. Rev.* A **79** 041401
[7] Petretti S, Vanne Y V, Saenz A, Castro A and Decleva P 2010 *Phys. Rev. Lett.* **104** 223001
[8] Gallup G A and Fabrikant I I 2010 *Phys. Rev.* A **81** 033417
[9] Chu X 2010 *Phys. Rev.* A **82** 023407
[10] Litvinyuk I V *et al* 2003 *Phys. Rev. Lett.* **90** 233003
[11] Alnaser A S *et al* 2004 *Phys. Rev. Lett.* **93** 113003
[12] Pavičić D, Lee K F, Rayner D M, Corkum P B and Villeneuve D M 2007 *Phys. Rev. Lett.* **98** 243001
[13] Meckel M *et al* 2008 *Science* **320** 1478
[14] Thomann I *et al* 2008 *J. Phys. Chem. A* **112** 9382
[15] Kumarappan V *et al* 2008 *Phys. Rev. Lett.* **100** 093006
[16] Staudte A *et al* 2009 *Phys. Rev. Lett.* **102** 033004
[17] Akagi H, Otobe T, Staudte A, Shiner A, Turner F, Dörner R, Villeneuve D M and Corkum P B 2009 *Science* **325** 1364
[18] Magrakvelidze M *et al* 2009 *Phys. Rev.* A **79** 033408
[19] von den Hoff P *et al* 2009 *Appl. Phys.* B **98** 659
[20] Stapelfeldt H and Seideman T 2003 *Rev. Mod. Phys.* **75** 543
[21] Talebpour A, Larochelle S and Chin S L 1998 *J. Phys. B: At. Mol. Opt. Phys.* **31** 2769
[22] Talebpour A, Bandrauk A D, Yang J and Chin S L 1999 *Chem. Phys. Lett.* **313** 789
[23] Bhardwaj V R, Rayner D M, Villeneuve D M and Corkum P B 2001 *Phys. Rev. Lett.* **87** 253003
[24] Bhardwaj V R, Corkum P B and Rayner D M 2004 *Phys. Rev. Lett.* **93** 043001
[25] McKenna J, Sayler A M, Gaire B, Johnson N G, Carnes K D, Esry B D and Ben Itzhak I 2009 *Phys. Rev. Lett.* **103** 103004
[26] Chu S I 2005 *J. Chem. Phys.* **123** 062207
[27] Otobe T and Yabana K 2007 *Phys. Rev.* A **75** 062507
[28] Son S K and Chu S I 2009 *Chem. Phys.* **366** 91
[29] Muth-Böhm J, Becker A and Faisal F H M 2000 *Phys. Rev. Lett.* **85** 2280
[30] Muth-Böhm J, Becker A, Chin S L and Faisal F H M 2001 *Chem. Phys. Lett.* **337** 313
[31] Kjeldsen T K, Bisgaard C Z, Madsen L B and Stapelfeldt H 2003 *Phys. Rev.* A **68** 063407
[32] Jaroń-Becker A, Becker A and Faisal F H M 2006 *Phys. Rev. Lett.* **96** 143006
[33] Tong X M, Zhao Z X and Lin C D 2002 *Phys. Rev.* A **66** 033402
[34] Zhao S F, Jin C, Le A T, Jiang T F and Lin C D 2010 *Phys. Rev.* A **81** 033423
[35] Zhao Z X, Tong X M and Lin C D 2003 *Phys. Rev.* A **67** 043404
[36] Kjeldsen T K and Madsen L B 2005 *Phys. Rev.* A **71** 023411
[37] Zhao S F, Jin C, Le A T, Jiang T F and Lin C D 2009 *Phys. Rev.* A **80** 051402
[38] Abu-samha M and Madsen L B 2010 *Phys. Rev.* A **81** 033416
[39] Zhao S F, Jin C, Le A T and Lin C D 2010 *Phys. Rev.* A **82** 035402
[40] Abu-samha M and Madsen L B 2010 *Phys. Rev.* A **82** 043413
[41] Zhang B and Zhao Z X 2010 *Phys. Rev.* A **82** 035401
[42] Kjeldsen T K, Bisgaard C Z, Madsen L B and Stapelfeldt H 2005 *Phys. Rev.* A **71** 013418
[43] Madsen C B and Madsen L B 2007 *Phys. Rev.* A **76** 043419
[44] Brabec T, Côté M, Boulanger P and Ramunno L 2005 *Phys. Rev. Lett.* **95** 073001
[45] Zhao Z X and Brabec T 2007 *J. Mod. Opt.* **54** 981
[46] Frisch M J *et al* 2003 *GAUSSIAN 03, revision B.04* (Pittsburgh, PA: Gaussian, Inc.)
[47] McFarland B K, Farrell J P, Bucksbaum P H and Gühr M 2008 *Science* **322** 1232
[48] Le A T, Lucchese R R and Lin C D 2009 *J. Phys. B: At. Mol. Opt. Phys.* **42** 211001
[49] Smirnova O, Mairesse Y, Patchkovskii S, Dudovich N, Villeneuve D, Corkum P and Ivanov M Yu 2009 *Nature* **460** 972